J Mater Sci (2014) 49:4180–4190
DOI 10.1007/s10853-014-8113-7

Electronic and phonon properties of the full-Heusler alloys X_2YAl (X = Co, Fe and Y = Cr, Sc): a density functional theory study

N. Arıkan · A. İyigör · A. Candan · Ş. Uğur · Z. Charifi · H. Baaziz · G. Uğur

Received: 25 October 2013 / Accepted: 11 February 2014 / Published online: 20 February 2014

Abstract First-principle calculations have been carried out on the structural, electronic, elastic, and phonon properties of the full-Heusler alloys X_2YAl (X = Co, Fe and Y = Cr, Sc). The calculations predict that the Fe_2CrAl and Co_2CrAl are half-metallic ferromagnets at the equilibrium lattice constant with a minority-spin energy gap of 0.2912 and 0.668 eV, respectively. Fe_2ScAl exhibit a gap in the majority density of states, with a few states at the Fermi level and about 0.217 states eV^{-1}, unlike the other Heusler compounds; due to this, it is considered a false half metal, and Co_2ScAl is considered a non-magnetic compound. The elastic constants were derived from the slopes of the acoustic branches in the phonon-dispersion curve. The calculated lattice constants, bulk modulus, and first-order pressure derivative of the bulk modulus are reported for the $L2_1$ structure and compared with previous values. Phonon-dispersion curves were obtained using the first-principle linear-response approach of the density-functional perturbation theory. The specific heat capacity at a constant volume C_V of X_2YAl (X = Co, Fe and Y = Cr, Sc) alloys is calculated and discussed.

N. Arıkan (✉)
Science Education Department, Education Faculty, Ahi Evran University, 40100 Kırşehir, Turkey
e-mail: nihat.arikan@hotmail.com

A. İyigör · A. Candan
Central Research and Practice Laboratory (AHİLAB), Ahi Evran University, 40100 Bağbaşı-Kırşehir, Turkey

Ş. Uğur · G. Uğur
Department of Physics, Faculty of Science, Gazi University, 06500 Ankara, Turkey

Z. Charifi · H. Baaziz
Department of Physics, Faculty of Science, University of M'sila, 28000 M'sila, Algeria
e-mail: charifizoulikha@gmail.com

Introduction

Heusler alloys have been of interest since their discovery in 1903 by Friedrich Heusler. It has been reported that it was possible to make ferromagnetic alloys from non-ferromagnetic constituents [1]. These ternary alloys are of the form X_2YZ, where Y and X are usually transitions metals, and Z is a main group element with s, p valence electrons (Al, In, Sb, Si, Ge, and Sn). The majority of these alloys form an $L2_1$ crystal structure with a face-centered cubic lattice (fcc). Further investigations indicated that the magnetic properties of these alloys are in relation with their chemical, $L2_1$ structure, and the ordering of the Y atoms on an fcc sublattice.

Recently, half-metallic ferromagnetic (HMFs) have attracted attention, as they showed great potential for spintronics, owing to tunneling magnetoresistance (TMR) and giant magnetoresistance (GMR) [2], and electromechanical [3] applications. Ever since De Groot et al., many more materials have been obtained both theoretically and experimentally to have HMFs properties. Apart from Heusler and half-Heusler alloys [4], half-metallic behavior has been found in perovskite structures [5], dilute magnetic semiconductors [6], some oxides [7], and materials possessing a zinc-blend structure [8, 9]. Many of the Heusler alloys of the X_2YZ stoichiometric composition are good candidates for devices based on a spin injection such as the GMR and the huge TMR in magneto electronic devices. They can also be used as perfect spin filters and spin-injection devices as an alternative to ferromagnetic 3d metals.

Despite the fact that about one hundred of full-Heusler alloys have been synthesized and investigated till date, the majority of all possible chemical compositions still waits for this realization. Iron- and cobalt-based Fe_2CrAl and Co_2CrAl alloys have been extensively studied using different theoretical and experimental methods [10–35]. Fe_2CrAl and Co_2CrAl alloys are more much suitable for wide technological applications because of their high Curie temperature, low coercivities, high-spin polarization, low saturation magnetization, and crystal structure compatibility. The electronic band structure, magnetism and transport properties, and formation energies of the Heusler X_2YAl (X = Fe, Co, Ni; Y = Ti, Cr) alloys using the full potential linearized augmented plane-wave (FP-LAPW) method have been studied [1, 17]. It has been shown that Cr sites carry large magnetic moments, and the moments at the Fe and Co sites are usually small, when compared with Ti substitution. All the densities of states are marked by a pseudogap that is to the left of the Fermi level, except for Fe_2AlTi, where the pseudogap is to the right of E_F. Among the selected materials, the Fe_2AlCr and Co_2AlCr alloys present a pronounced half metallicity character. The experimental results of the optical, electrical, magnetic properties, electronic structure, and the calculated optical spectrum of Fe_2TiAl, Fe_2Val, and Fe_2CrAl alloy have been also presented by Shreder et al. [12]. They found a drastic transformation of the band spectrum, especially near the Fermi level, when one Y element (Y = Ti, V, and Cr) replaces another. These changes are closely related to the magnetic properties of the Fe_2MeAl alloys and accompanied by a drastic change in the electrical and optical properties of these materials. The structural and magnetic properties of the Fe_2CrAl alloy have been measured using Mössbauer spectroscopy by Paduani et al. [14] and Lakshmi et al. [15], and using X-ray powder diffraction (XRD), and conducting quantum interface device (SQUID) magnetometer and a vibrating sample magnetometer (VSM) by Umetsu et al. [16]. The Mossbauer spectra showed the co-existence of a paramagnetic part with a magnetic hyperfine portion at all recorded temperatures. The confirmed crystal structures of the Fe_2CrAl alloy were single phases of A2, B2, and $L2_1$, depending on the quenched temperature. The values of the spontaneous magnetic moment, (I_S), and the curie temperature (T_C) of the A2 phase were 2.2 μ_B/f.u. and 316 K, and those of the B2 phase were 2.1 μ_B/f.u. and 265 K, respectively, which were larger than those of the $L2_1$-type phase of 1.6 μ_B/f.u. and 191 K.

For the Co_2CrAl alloy, electronic and magnetic properties were studied by several groups [18–22]. It is found to be perfectly half-metallic (HM), and a transition pressure of 75 GPa is obtained from HM to metal. The substitution of Cr for Co leads to a high-antibonding peak above E_F in the majority-spin band, while the energy gap in the minority-spin band is retained. With an increase in Cr content, the total spin moment decreases linearly from 3 μ_B/f.u. to zero, which obeys the Slater–Pauling curve quite well. The structural, microstructural, and magnetic properties of the Co_2CrAl thin film were investigated by Dubowik et al. [23] using selective-area microdiffraction of a transmission microscope (TEM) and a SQUID magnetometer. Their measurements show that the films with the best $B2/L2_1$ structure exhibit a ferromagnetic order below the curie temperature T_C = 330–340 K and below 200 K, they exhibited magnetic characteristics suggesting the presence of antiferromagnetic ordering. The calculated electronic band structure and transport properties of the Co_2CrAl alloy, with a full-Heusler ($L2_1$) structure, were studied and it is suggested to be a half-metallic ferromagnet (HMF) with a magnetic moment of 3 μ_B per formula unit and a spin-flip gap of 0.181 eV [24, 25, 27].

It is very interesting to have a look at those compounds that are missing from the series of X_2ScAl Heusler compounds. Neither the compound Co_2ScAl nor Fe_2ScAl is reported in any experiment. Electronic band structure calculations for X_2YZ Heusler compounds are presented [30]. Among the interesting aspects of the electronic structure of the materials are the contributions from both X and Y atoms to the total magnetic moment. It is found that the total magnetic moment also depends on the kind of Z atoms, although they do not directly contribute to it. Co_2ScAl has 24 valence electrons, and the magnetic moment vanishes at all sites; however, in Co_2ScSi, the Co_2 sub-lattice starts ordering ferromagnetically, whereas the Sc atoms do not contribute to the magnetic moment. In addition, the magnetic moment of Co is changing with the exchange of Al by Si. In order to find the stable magnetic configuration and the optimized lattice constant of Co_2YAl (Y = Sc, Ti, V, Cr, Mn, and Fe) Heusler alloys, Rai et al. [36] performed the total-energy calculations of Co_2YAl (Y = Sc, Ti, V, Cr, Mn, and Fe) Heusler alloys based on the generalized gradient approximation (GGA) within the FP-LAPW method. A study of the thermo-chemical stability and magnetism of 810 possible full-Heusler alloys using a rigorous computational search based on the density-functional theory have been performed [37]. It is found that some of them are candidates for itinerant ferromagnetism with 100 % spin polarization, and about 56 % of the calculated phases appear to be ferromagnetic with a magnetic moment larger than 0.5 μ_B. Although the saturation moments may reach a maximum value of approximately 7.5 μ_B, a value of 1.91 μ_B for the magnetic moment of Fe_2ScAl alloys is found.

Although considerable progress has been made in theoretically describing the structural and electronic properties of Fe_2CrAl and Co_2CrAl alloys, many of their dynamical

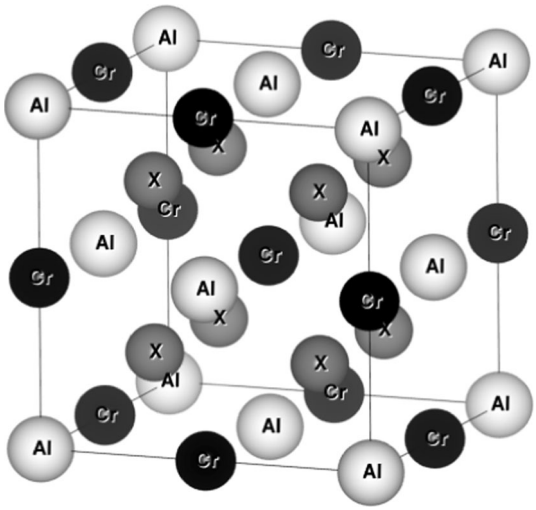

Fig. 1 Crystal structure of the full-Heusler alloys X_2YZ

properties are still not well established. To the best of our knowledge, the structural, elastic, electronic, and phonon properties of Co_2ScAl and Fe_2ScAl in the $L2_1$ phase have not been studied using the density-functional theory. The full phonon-dispersion curves are necessary for a microscopic understanding of the lattice dynamics. Knowledge of the phonon spectrum plays a significant role in determining many material properties such as phase transition, thermodynamic stability, transport and thermal properties, and electron–phonon interactions. Thus, the aim of this work is to investigate the structural, elastic, and electronic properties with interchanging elements at the X and Y positions of X_2YAl (X = Co, Fe and Y = Cr, Sc) Heusler alloys by employing the plane-wave pseudopotential method. These results are used, within a linear-response approach, to calculate the phonon-dispersion curves and the density of states (DOS). This article is organized as follows. In Sec. II, we describe our calculational methods, and Sec. III is devoted to the discussion of the results of our calculations for the structural and vibrational properties of X_2YAl (X = Co, Fe and Y = Cr, Sc) Heusler alloys, including a comparison with previous available works. The electronic structure of these alloys is examined. A conclusion is provided in Sec. IV.

Structure and method of calculation

Most of the full-Heusler alloys X_2Y Z often crystallize in the cubic $L2_1$ structure (space group Fm-3 m). Generally, X and Y atoms are transition metals, and Z is a main group element. In some cases, Y is replaced by a rare earth element. The X atoms are placed on 8a (1/4, 1/4, 1/4), and the Y and Z atoms are placed on 4a (0, 0, 0) and 4b (1/2, 1/2, 1/2) Wyckoff positions, respectively. The cubic $L2_1$ structure consists of four inter-penetrating fcc sub-lattices, two of which are equally occupied by X. The two X fcc sub-lattices combine and form a simple cubic sub-lattice. The Y and Z atoms occupy, alternately the center of the simple cubic X_2 sub-lattice, resulting in a CsCl-type super structure (see Fig. 1).

The calculations were performed using a plane-wave pseudopotential scheme within the density-functional theory (DFT) as implemented in the Quantum-ESPRESSO package [38]. The electronic exchange–correlation potential was calculated by the GGA as parametrized by Perdew–Burke–Ernzerhof (PBE) [39]. The wave functions were expanded in a plane-wave basis set with a kinetic energy cut-off of 40 Ry. Brillouin-zone integrations were performed using a 10 × 10 × 10 k-point mesh. Integration up to the Fermi surface was performed using the smearing technique [40] with a smearing parameter $\sigma = 0.02$ Ry. Having obtained self-consistent solutions of Kohn–Sham equations, the lattice-dynamical properties were calculated within the framework of the self-consistent density-functional perturbation theory [41, 42]. To find complete phonon dispersions and DOS, eight dynamical matrices were calculated on a 4 × 4 × 4 q-point mesh. The dynamical matrices at arbitrary wave vectors were evaluated using Fourier deconvolution on this mesh. Specific heat at constant volume is calculated at various temperatures from the phonon frequencies obtained through the quasi-harmonic Debye model (QHA) [43].

Elastic constants were obtained from the slopes of the acoustic branches in the phonon-dispersion curves [44]. The sound velocities correspond to the small-wavelength behavior of the acoustic phonons. These velocities are associated with C_{11}, C_{44}, and C_{12} by [44]

$$\upsilon_{\mathrm{LA}}^{[001]} = \sqrt{C_{11}/\rho} \tag{1}$$

$$\upsilon_{\mathrm{TA}}^{[001]} = \sqrt{C_{44}/\rho} \tag{2}$$

$$\upsilon_{\mathrm{LA}}^{[110]} = \sqrt{(C_{11} + C_{12} + 2C_{44})C_{11}/\rho}, \tag{3}$$

where ρ is the mass density of the X_2YAl (X = Co, Fe and Y = Cr, Sc) Heusler alloy.

Results and discussion

Ground-state properties and determination of elastic constants

Spin-polarized total energies were calculated as a function of lattice constant for X_2YAl (X = Co, Fe and Y = Cr, Sc) Heusler alloys and were fitted to the Murnaghan's equation

Table 1 Calculated lattice constant a (Å), bulk modulus B (GPa), the total magnetic moment M_t (μ_B), and elastic constants C_{ij} (GPa), for X_2YAl (X = Co, Fe and Y = Cr, Sc) full-Heusler alloys, compared with the available experimental and theoretical data

	a	M_t	B	C_{11}	C_{12}	C_{44}	B/G
Fe_2CrAl							
This work	5.65	1.01	177.46	229.56	151.41	275.94	0.979
CASTEP (GGA) [10]	–	–	201.08	289.75	156.75	153.07	1.886
CASTEP (LDA) [10]	–	–	177.09	258.24	134.78	139.14	1.785
Exp. [12]	5.811						
Exp. [13]	5.800						
Exp. [27]	5.800						
Exp. [15]	5.807						
Exp. [14]	5.811	1.51					
Exp. [16]	5.789						
FP-LAPW nm [17]	5.654	–	225.00				
FP-LAPW fm [17]	5.654	–	229.00				
FSKKR [33]	–	0.91					
Co_2CrAl							
This work	5.71	3.00	328.40	355.82	314.69	417.86	1.268
FP-LAPW nm [17]	5.693	–	208.00				
FP-LAPW fm [17]	5.714	–	204.00				
FSKKR [33]	–	2.95					
KKR [34]	–	2.99					
Exp. [18]	5.5726						
Exp. [30]	5.727	1.55					
FLAPW [19]	5.70	3.00	207.23				
FLAPW [30]		3.00					
Exp. [26]	5.75						
Fe_2ScAl							
This work	6.012	1.92	127.40	280.14	51.03	120.03	1.081
[50]	6.006	1.91					
Co_2ScAl							
This work	5.961	0	168.23	180.16	162.26	150.86	1.787
[36]	6.320						
[30]	5.960						
[50]	5.957	0					

of state [45] to obtain the basic ground-state properties. It was also well-proved that the ferromagnetic configuration is lower in energy than the non-magnetic case for the studied compounds except for the Co_2ScAl alloy, which is found to be a non-magnetic compound. Measurements of the temperature and field dependence of the magnetization and the *ac* susceptibility show that Fe_2CrAl is a ferromagnet with $T_C = 246$ K [12]. The calculated lattice constants and bulk modulus of X_2YAl (X = Co, Fe and Y = Cr, Sc) alloys are presented in Table 1. Comparing the experiments and theoretical data [10, 12–18, 26, 27, 30, 33, 34], the maximum deviation in the lattice constant is 2 % for Fe_2CrAl, and the minimum deviation is around 0.3 % for the Co_2CrAl alloy. The optimized lattice parameters were in excellent agreement with other theoretical studies [30, 36] but less those that found in [36] for Co_2ScAl. It is observed that the lattice constant decreases by about 0.8 %, when the Fe atom is replaced by the Co atom in X_2ScAl alloys and increases by 1 % in X_2CrAl alloys. It should be mentioned that the bulk modulus of Co_2CrAl is the largest and is about 328.40 GPa; as a result, it is predicted to be the hardest one in the studied compounds. On the other hand, the bulk modulus increases by 85 % when Fe is replaced by Co in X_2CrAl alloys and by −32 % in X_2ScAl alloys. However, when we replace Cr by Sc in Co_2YAl, it decreases by 49 %.

Our calculations show that Fe_2CrAl and Co_2CrAl have total magnetic moments of 1.01 and 3 μ_B per formula unit, respectively, which is equal to an integer number of μ_B expected for an HMF. This is in excellent agreement with the Slater–Pauling rule and is confirmed by several studies [17, 24, 25, 27, 30, 46, 47]. It is found that Co_2CrAl has local magnetic moments of about 0.7–0.85 μ_B on Co and in a range of 1.44–1.54 μ_B on Cr. The exchange interactions

between the Co(Fe) and Cr atoms are found to be ferromagnetic, leading to a total calculated moment of 3.0 (1.0) μ_B [11, 31]. In general, the Y atoms, and in some cases, also the X atoms carry the magnetic moments. However, in the compounds that contain Cr atoms, it has been shown that Cr sites carry large magnetic moments, and the moments at the Al sites are usually small [17]. The direction of the spin polarization of Al is antiparallel to the others. The replacement of Fe by Co in the studied alloys leads to a substantial increase in the magnetic moment from 1 to 3 μ_B. In the present study, the Co_2ScAl Heusler alloy does not show any magnetic moment. This is explained by the fact that Co_2ScAl has 24 valence electrons, and the magnetic moment vanishes at all sites. The result is a vanishing total magnetic moment as expected from the Slater–Pauling rule. It has also been found that the total magnetic moment depends on the type of *Z* element, although they do not directly contribute to it. In Co_2 compounds, the replacement of Al by Si or an exchange between other members of the 3*A* and 4*A* groups plays an important role in the distribution of electrons in the various symmetry distinguished states (t_{2g} and e_g) at Co as well as at *B* sites [30]. However, the other compound Fe_2ScAl has a moderate magnetic moment of about 1.92 μ_B per formula unit, which is far less than the predicted one of 2 μ_B using the Slater–Pauling rule. This is an indication that Fe_2ScAl is not a perfectly half-metallic compound, because the total spin moment is not an integer number. We find that the total magnetic moment per formula unit increases when we move from Co_2ScAl to Fe_2ScAl.

Elastic constants are known as numbers that quantify the response of a particular material to elastic or non-elastic deformation when a stress load is applied to that material. The elastic constants of solids provide valuable information on their dynamical and mechanical properties. In particular, they provide information on the stiffness and stability of materials. Various experimental techniques are available for the measurement of elastic constants such as neutron scattering, ultrasonic wave propagation, and Brillouin scattering.

An efficient way of calculating elastic constants is important, because these constants are directly employed in practical uses of materials. Calculation of the elastic constants at given temperatures can also serve as a measure of the reliability of the interatomic potential at those temperatures. The elastic constants of the full-Heusler alloys X_2YAl (X = Co, Fe and Y = Cr, Sc) are calculated using the approximation reported in [48]. They are listed in Table 1, along with the data available from other calculations for a comparison [10]. Our calculated elastic constants C_{12} and C_{11} of Fe_2CrAl are in excellent agreements with those calculated with the same method incorporated in Castep code [10]. Unfortunately, the experimental and theoretical values of the elastic constants for Co_2CrAl, Co_2ScAl, and Fe_2ScAl materials are not available in the literature. Thus, further experimental studies are needed to compare with these computed results for Co_2CrAl, Co_2ScAl, and Fe_2ScAl. In addition, it should be mentioned that the elastic constants increase as we replace Fe with Co in these Heusler alloys except for C_{11} which decreases when we progress from Fe_2ScAl to Co_2ScAl. The mechanical stability of these compounds has been analyzed in terms of their elastic constants. For cubic crystals, the conditions for mechanical stability are given by [49]

$$C_{44} > 0,\ \ (C_{11} - C_{12})/2 > 0 \text{ and}$$
$$B = (C_{11} + 2C_{12})/3 > 0.$$

These criteria are verified (see Table 1), so it is concluded that all compounds are stable in the $L2_1$ phase. According to the ratio *B/G,* Fe_2CrAl, Co_2CrAl, and Fe_2ScAl are brittle, whereas Co_2ScAl is ductile.

Density of states and electronic band structure

We present the spin-dependent energy bands of X_2YAl (X = Co, Fe and Y = Cr, Sc) along high-symmetry directions in the Brillouin zone, as presented in Fig. 2. The Fermi level E_F shown by a broken horizontal line intersects the E(k) curves in the majority (up)-spin state but is located at the energy gap in the minority (down)-spin state for Fe_2CrAl and Co_2CrAl. It is obvious that the majority-spin electrons are metallic, whereas there is an energy gap of about 0.2912 and 0.668 eV around the Fermi level in the bands for the minority-spin electrons for Fe_2CrAl and Co_2CrAl alloys, respectively. This suggests that Fe_2CrAl and Co_2CrAl are half metals (HM), and electrons at the Fermi level are 100 % spin polarized. The spin-flip gaps are 0.2188 and 0.0424 eV for Fe_2CrAl and Co_2CrAl alloys, respectively. The non-zero spin-flip gap implies that Fe_2CrAl and Co_2CrAl are true HMF. The size of the gap increases if Fe is replaced by Co; however, the spin-flip gap decreases. We find that Fe_2ScAl exhibit a gap in the majority DOS, with a few states at the Fermi level being about 0.217 states eV^{-1} unlike the other Heusler compounds. The reason is that Fe_2ScAl has only 22 valence electrons, that is, less than 24; therefore, we can consider it a false half metal. In addition, on replacing Fe by Co, in the compound X_2ScAl, Co_2ScAl becomes metallic.

The band gap in the minority bands basically arises from the covalent hybridization between the d states of the Co(Fe) and Cr atoms, leading to the formation of bonding and antibonding bands with a gap in between. This covalent hybridization is the reason for the formation of bonding and antibonding states and determines the position of E_F. The majority DOS at E_F is lower in Fe_2CrAl (2.98791 states eV^{-1}) as compared with the Co_2CrAl

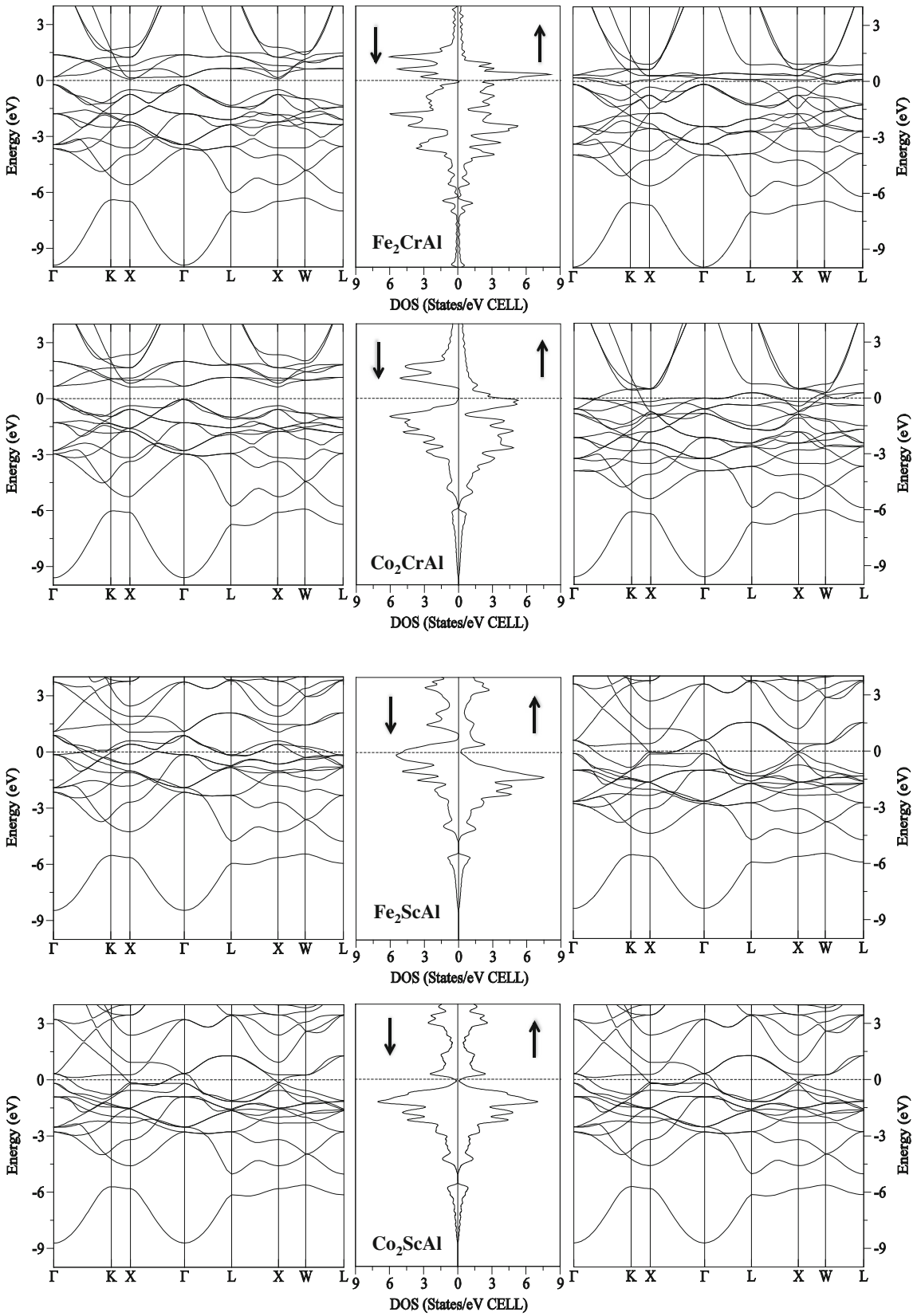

Fig. 2 Calculated minority spin, majority spin-band structure, and total DOS for X_2YAl (X = Co, Fe and Y = Cr, Sc) Heusler alloys

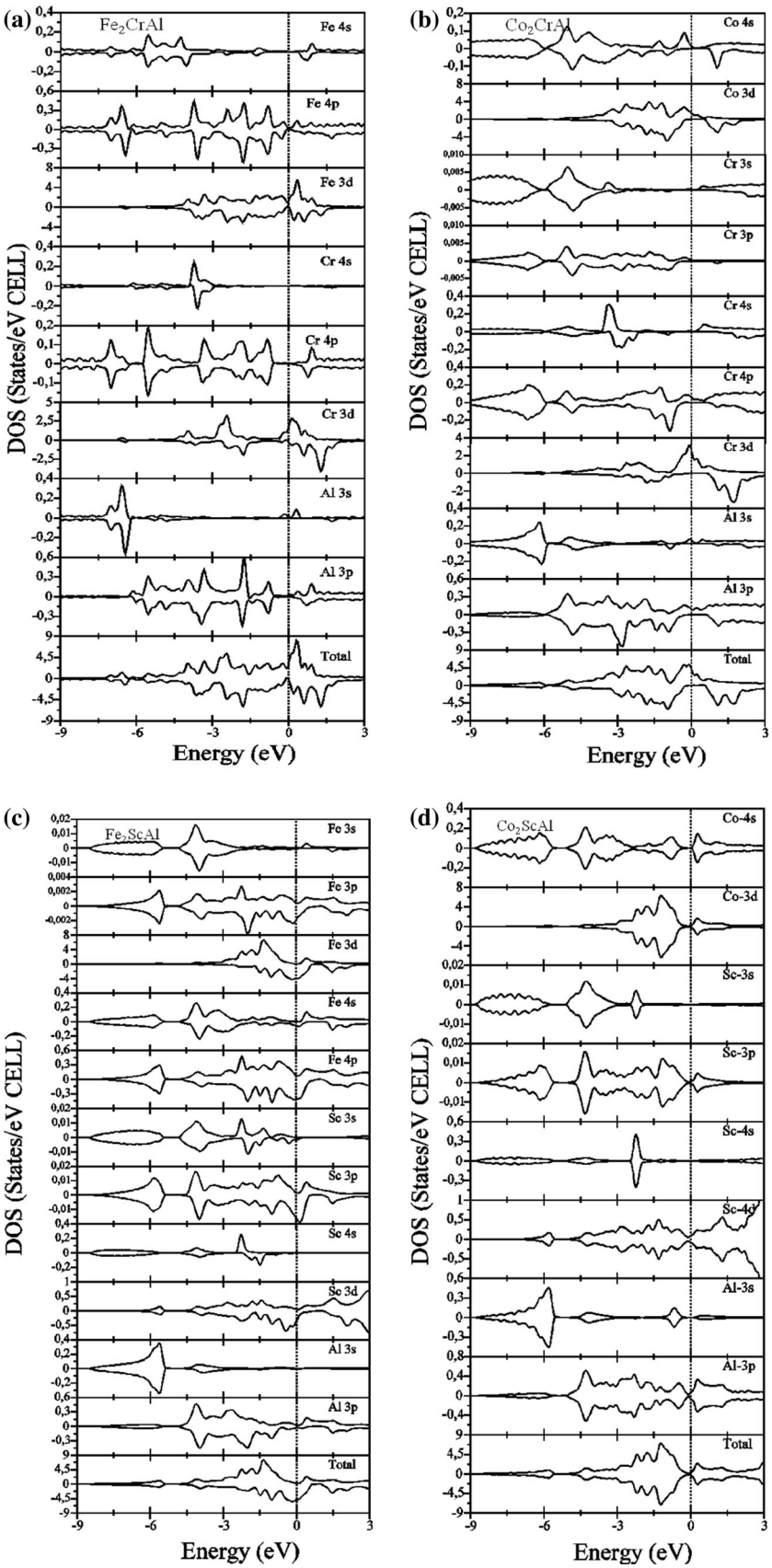

Fig. 3 The total and partial DOS of **a** Fe_2CrAl **b** Co_2CrAl **c** Fe_2ScAl **d** Co_2ScAl **e** and **f** total DOS of X_2CrAl and X_2ScAl (X = Co, Fe) Heusler alloys

compound (4.166 states eV^{-1}). The main characters of our results are similar with previous investigations of electronic structure [10–12, 18–22].

In order to further study the electronic structure of these alloys, in Fig. 3a, b, we present the spin-projected partial DOS of Fe_2CrAl and Co_2CrAl. The lowest valence bands in the energy region that is lower than −6 eV in both the majority and minority spin states are mainly due to the ''s'' electrons of the Al atom. In addition, the band structure is almost identical for both spin directions. The low-energy part around −5 eV mainly consists of the p states of Al, which hybridize with the p and d states of the Cr and Fe(Co) atoms, and the energy region between −3 and 2 eV mainly forms the d electrons of the Fe(Co) and Cr atoms. The states of the 3d atoms extend from about −5 to +2 eV and hybridize with each other. The d states are wide on an energy scale, which may result from the strong hybridization between the Fe(Co) and Cr atoms. The upper dispersed bands are due to the strong hybridization of Cr d and Co d electrons, including a contribution from Al p states in the occupied valence states. The detailed analysis shows important changes of DOS (see Fig. 3e, f) in the vicinity of the Fermi level while moving from Fe_2CrAl to Co_2CrAl and in the minority states of X_2ScAl alloys. The addition of an extra electron, by the change from Fe to Co in X_2CrAl, again leads to a shift of the Fermi level to lower energies, but it is still in the gap for the spin minority DOS and to a partial occupation of the conduction band. The character of the band states for Co_2ScAl has been identified by calculating its total and partial DOS (in Fig. 3d). It is shown that there is no gap at the Fermi level and the total DOS, which is 0.329 states eV^{-1} cell for Co_2ScAl, indicates that the system is metallic and non-magnetic. The results indicate that the predominant contributions of the DOS at the Fermi level come from the Co *3d*, Sc *4d,* and Al *3p* states for Co2ScAl. In addition, from the calculated total DOS of Co2ScAl alloys, it can be seen that there are some peaks below and above the Fermi level. Those peaks are mainly dominated by the Co *3d* state. The majority DOS at E_F in Fe_2ScAl is (0.217 states eV^{-1}), and the minority one is (4.962 eV states eV^{-1}); the main contribution around the Fermi level comes from the d-Fe states.

Phonon properties and specific heats

Phonon-dispersion curves calculated for the $L2_1$ phase Heusler alloys X_2YAl (X = Co, Fe and Y = Cr, Sc) are shown in Fig. 4. Since primitive cells of X_2YAl (X = Co, Fe and Y = Cr, Sc) contain four atoms, the corresponding number of vibration modes is twelve, as seen in Fig. 4, of which three are acoustic branches and the remaining nine are optical modes. We have not observed any phonon anomaly in the phonon DOS for Fe_2ScAl and Co_2ScAl alloys. We do not find any imaginary phonon frequency in the whole Brillouin zone for X_2YAl (X = Co, Fe and Y = Cr, Sc) alloys. This supports the dynamical stability of X_2YAl (X = Co, Fe and Y = Cr, Sc) in the Heusler structure. The contribution of the heavier atoms to the total DOS is dominated at low frequencies, and that of the lighter atoms is important at high frequencies (see Fig. 4, right panel). The three highest optical phonon modes of these materials have a major amplitude contribution to Al atoms. At the Γ point, there are threefold degenerate optical modes, as there are four atoms in the unit cell. For Fe_2CrAl, Co_2CrAl, and Co_2ScAl, gaps exist between optical and optical phonon branches. In the phonon DOS, the band gap between the optical and optical branches of Fe_2CrAl, Co_2CrAl, and Co_2ScAl is around 0.959, 2.128, and 0.47 THz, respectively. For Fe_2ScAl, there is no gap between the optical and optical phonon branches in Fig. 4, as there is a considerable overlap between the optical phonon branches. The optical mode frequencies at the τ point are 10.210, 8.872, and 6.683 THz for Fe_2CrAl; 10.192, 7.255, and 7.141 THz for Co_2CrAl; 6.407, 7.900, and 9.526 for Co_2ScAl; and 4.419, 8.752, and 9.485 THz for Fe_2ScAl, respectively. Due to lack of experimental results, the calculated phonon curves could not be compared. The phonon calculations of these materials will certainly be useful for the interpretations of future theoretical and experimental studies. We observed phonon anomalous along with τ-K and τ-L directions at TA_2 (acoustic transverse) branches for Co_2ScAl and Fe_2CrAl. The origin of phonon anomalous in Ni_2MnGa has been investigated by first-principle calculations [51]. It has been found that the Raman-active optical modes lower their energy due to the negative force constants, by which the acoustic mode TA_2 becomes unstable due to the repulsive interaction with the anomalous optical mode. This acoustic-optical interaction might be of more general interest than just for the Heusler compounds [51]. We can conclude that the anomalous for Co_2ScAl and Fe_2CrAl is connected with the acoustic–optical interaction.

The heat capacity, *C*, of a material is a fundamental state property of matter, as it measures the ability of a substance that can store heat energy. It is described by the ratio of the energy *dE* transferred to a substance to raise its temperature by an amount *dT*. The specific heat of a material is closely related to its vibrational and configurational entropy, which is mostly affected by nearest-neighbor configurations. First-principle calculations combined with the quasi-harmonic approximation (QHA) have been employed to predict the temperature dependence of the vibrational contributions to the specific heat capacity at a constant volume (C_V) of X_2YAl (X = Co, Fe and Y = Cr, Sc) alloys. The results are illustrated in Fig. 5. It can be seen that the rapid increase in the specific heat is a marked

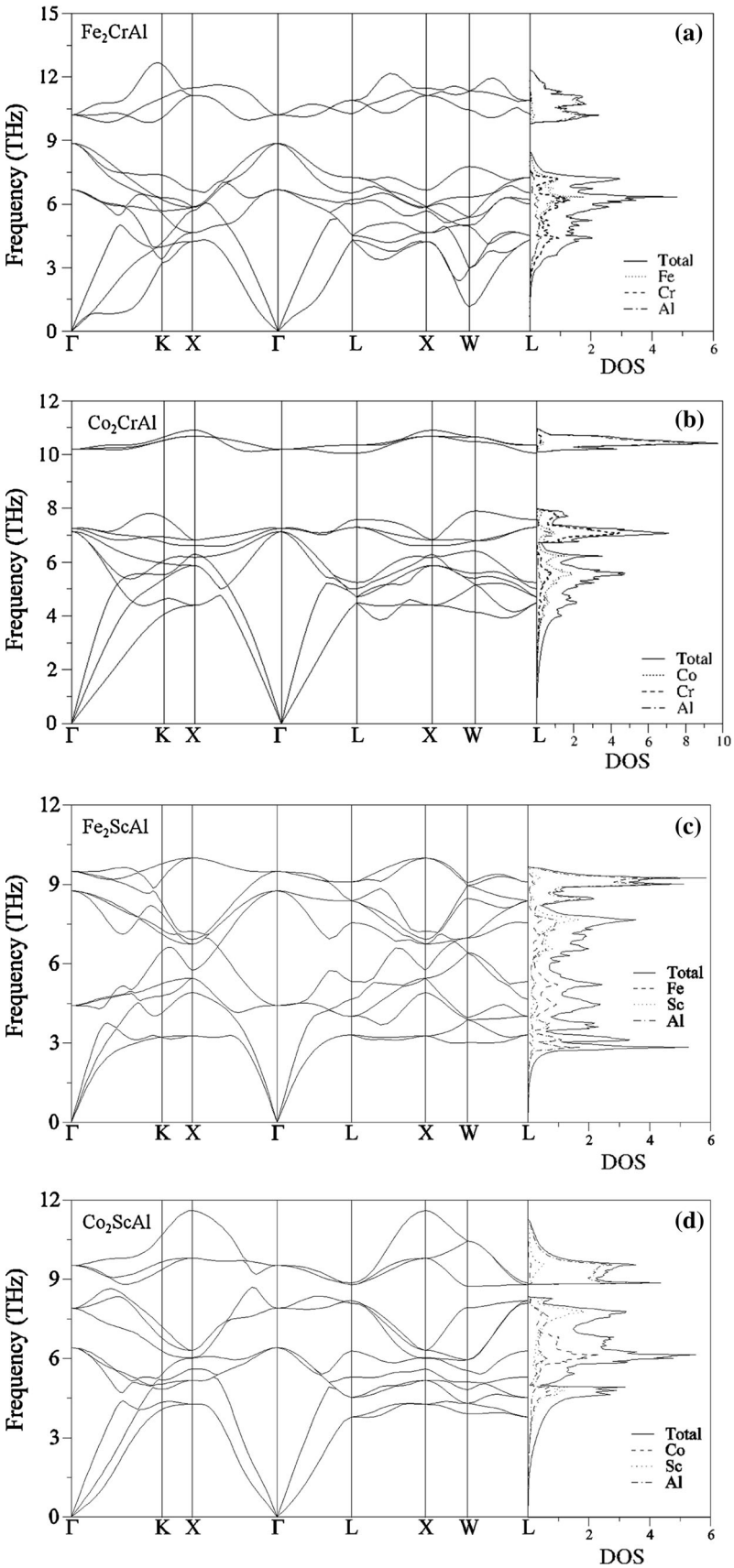

Fig. 4 Calculated phonon-dispersion curves and phonon DOS for **a** Fe_2CrAl **b** Co_2CrAl **c** Fe_2ScAl **d** Co_2ScAl Heusler alloys along several high-symmetry lines in the Brillouin zone

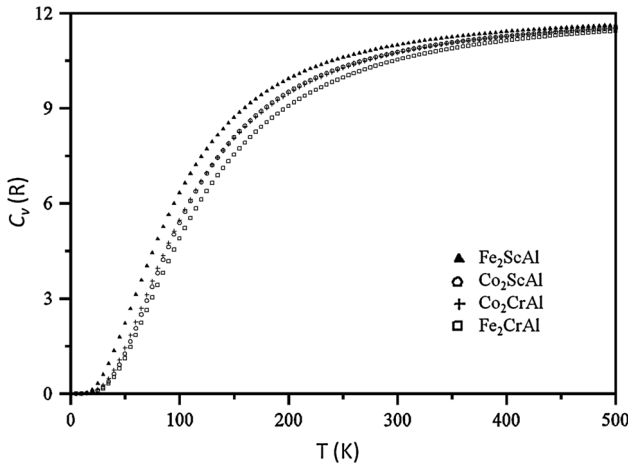

Fig. 5 The temperature dependence of the specific heat capacity at constant volume (C_V) of X_2YAl (X = Co, Fe and Y = Cr, Sc) Heusler alloys

feature of these alloys; when the temperature reaches about 1000 K, C_V becomes constant following the Dulong–Petit law. Unfortunately, no experimental data are available for the specific heat capacity for these materials. No effect is shown on C_V by exchanging Cr by the Sc atom in Co_2YAl alloys.

Conclusion

The structural, electronic, magnetic, and phonon properties of Heusler alloys X_2YAl (X = Co, Fe and Y = Cr, Sc) have been investigated using the pseudopotential plane-wave method. The exchange–correlation potential is treated using the GGA. The main focus of this work is to study the structural, electronic, elastic, and phonon properties of X_2YAl (X = Co, Fe and Y = Cr, Sc) and to elaborate the changes brought about in the studied properties of X_2YAl (X = Co, Fe and Y = Cr, Sc) by replacing the Fe atom by Co atom and the Cr atom by the Sc atom. The half metallicity and the stability of the ferromagnetic state have been investigated. The band structure calculation shows that Co_2CrAl and Fe_2CrAl are true half-metallic ferromagnets with a magnetic moment of 3 and 1 μ_B per formula unit, respectively, which is characterized by an indirect band gap of about 0.2912 and 0.668 eV for Fe_2CrAl and Co_2CrAl, respectively, at around the Fermi level in the minority-spin band. However, Fe_2ScAl is found to be a false half metal with a false gap in the majority of the spin states. The calculated total spin magnetic moments of all the compounds are found to be in good agreement with other theoretical calculations and in good agreement with the Slater–Pauling rule. Spin-polarized electronic structure calculations show that the moments are mainly of 3*d* origin. The minority density of states is exactly zero at the Fermi energy, whereas the majority *d* density of states can have a peak or a valley close to E_F. The slope of acoustic phonon-dispersion curves was used to calculate elastic constants C_{ij}. Elastically, all the compounds have been found to be stable in the $L2_1$ phase. The DOS of the minority-spin band as well as of the majority-spin band is affected by replacing Fe by Co. The main change is a small shift of the minority DOS to higher energies and the majority DOS to lower energies with regard to the Fermi level for X_2CrAl alloys. The phonon frequencies and phonon densities of states in the $L2_1$ phase in several lines of high symmetry of the Brillouin zone were obtained and discussed using the density-functional perturbation theory. Finally, the specific heat capacity at constant volume C_V of X_2YAl (X = Co, Fe and Y = Cr, Sc) alloys is calculated and discussed.

Acknowledgements This work was supported by the Gazi University Research Project Unit under Project No 05/2012-07, 05/2012-08, 05/2012-62, 05/2012-63 and the Ahi Evran University Research Project Unit under Project No. PYO.EGF.4001.13.002.

References

1. Heusler F (1903) "Über magnetische Manganlegierungen" Verhandlungen der Deutschen Physikalischen Gesellschaft (in German) 5:219
2. Žutić I, Fabian J, Sarma SD (2004) Spintronics: fundamentals and applications. Rev Mod Phys 76:323–410
3. Wolf SA, Treger D (2000) Spintronics: a new paradigm for electronics for the new millennium. IEEE Trans Magn 36(5):2748–2751
4. de Groot RA, Mueller FM, van Engen PG, Buschow KHJ (1983) New class of materials: half-metallic ferromagnets. Phys Rev Lett 50:2024–2027
5. Kobayashi K-I, Kimura T, Sawada H, Terakura K, Tokura Y (1998) Room-temperature magnetoresistance in an oxide material with an ordered double-perovskite structure. Lett Nat 395: 677–680
6. Ono K, Okabayashi J, Mizuguchi M, Oshima M, Fujimori A, Akinaga H (2002) Fabrication, magnetic properties, and electronic structures of nanoscale zinc-blende MnAs dots. J Appl Phys 91:8088–8092
7. Schwarz K (1986) CrO_2 predicted as a half-metallic ferromagnet. J Phys F Met Phys 16:L211–L215
8. Xie W-H, Xu Y-Q, Liu B-G (2003) Half-metallic ferromagnetism and structural stability of zincblende phases of the transition-metal chalcogenides. Phys Rev Lett 91:037204–037207
9. Shoren H, Ikemoto F, Yoshida K, Tanaka N, Motizuki K (2001) First principles electronic band calculation of (Zn, Cr)Te, (Zn, Cr)Se and (Zn, Cr)S. Phys E 10:242–246
10. Niu XL, Wang LJ (2012) Effect of transition-metal substitution on electronic and mechanical properties of Fe_3Al: first-principles calculations. Comput Mater Sci 53:128–132
11. Zhang M, Brück E, de Boer FR, Wu G (2004) Electronic structure, magnetism, and transport properties of the Heusler alloy Fe_2CrAl. J Magn Magn Mater 283:409–414

12. Shreder E, Streltsov SV, Svyazhin A, Makhnev A, Marchenkov VV, Lukoyanov A, Weber HW (2008) Evolution of the electronic structure and physical properties of Fe_2MeAl (Me = Ti, V, Cr) Heusler alloys. J Phys Condens Matter 20:045212
13. Mizutani S, Ishida S, Fujii S, Asano S (2007) Half-metallicity and stability of ferromagnetism in $(Fe_{1-x}Co_x)_2CrZ$ (Z = s, p elements). Mater Trans 48:748–753
14. Paduani C, Pöttker WE, Ardisson JD, Schaf J, Takeuchi AY, Yoshida MI, Soriano S, Kalisz M (2007) Mössbauer effect and magnetization studies of the $Fe_2 + xCr_1 - xAl$ system in the $L2_1$ (X_2YZ) structure. J Phys Condens Matter 19:156204
15. Lakshmi N, Venugopalan K, Varma J (2002) Mössbauer studies of hyperfine fields in disordered the Fe_2CrAl. Pramana J Phys 59(3):531–537
16. Umetsu RY, Morimoto N, Nagasako N, Kainuma R, Kanomata T (2012) Annealing temperature dependence of crystal structures and magnetic properties of Fe_2CrAl and Fe_2CrGa Heusler alloys. J Alloy Compd 528:34–39
17. Kellou A, Fenineche NE, Grosdidier T, Aourag H, Coddet C (2003) Structural stability and magnetic properties in X_2AlX' (X = Fe Co, Ni;X' = Ti, Cr) Heusler alloys from quantum mechanical calculations. J Appl Phys 94(5):3292–3298
18. Kim KW, Hyun YH, Park SY, Lee YP, Rhee JY, Kudryavtsev YV, Oksenenko VA, Dubowik J (2008) Electronic structures and magnetic properties of Co_2CrAl films. J Korean Phys Soc 53(5):2475–2478
19. Ram S, Chauhan MR, Agarwal K, Kanchana V (2011) Ab initio study of Heusler alloys Co2XY (X = Cr, Mn, Fe; Y = Al, Ga) under high pressure. Philos Mag Lett 91(8):545–553
20. Dai X, Joudan M, Felser C (2009) High spin polarization in Co_2CrAl–Cr super lattice. J Phys D Appl Phys 42:084014
21. Luo H, Ma L, Zhu Z, Wu G, Liu H, Qu J, Li Y (2008) Ab initio study of Cr substitution for Co in the Heusler alloy Co_2CrAl: half-metallicity and adjustable magnetic moments. Phys B 403:1797–1802
22. Rai DP, Shankar A, Sandeep, Ghimire MP, Thapa RK (2012) Electronic structure and magnetic properties of Co_2YZ(Y = Cr, Z = Al, Ga) type Heusler compounds: a first principle study. Int J Mod Phys B 26(08):1250071–1250082
23. Dubowik J, Gościańska I, Kudryavtsev YV, Oksenenko VA (2007) Structure and magnetism of Co_2CrAl Heusler alloy films. Mater Sci Pol 25(4):1281–1287
24. Ishida S, Kawakami S, Asano S (2004) Theoretical predict of half-metals in Co–Cr–Fe–Al alloys. Mater Trans 45(4):1065–1069
25. Zhang M, Liu Z, Hu H, Liu G, Cui Y, Chen J, Wu G, Zhang X, Xiao G (2004) Is Heusler compound Co_2CrAl a half-metallic ferromagnet: electronic band structure, and transport properties. J Magn Magn Mater 277:130–135
26. Ko V, Han G, Qiu J, Feng YP (2009) The band structure-matched and highly spin-polarized CoCrZ/CuCrAl Heusler alloys interface. Appl Phys Lett 95(20):202502–202503
27. Buschow KHJ, Engen PG (1981) Magnetic and magneto-optical properties of Heusler alloys based on aluminium and gallium. J Magn Magn Mater 25(1):90–96
28. Cai Y, Bai Z, Yang M, Feng YP (2012) Effect of interfacial strain on spin injection and spin polarization of Co_2CrAl/NaNbO3/Co_2CrAl magnetic tunneling junction. EPL 99(37001):1–5
29. Hoshino T, Fujima N, Asato M, Tatsuoka H (2010) Ab-initio calculations for defect energies in Co_2MnSi and Co_2CrAl. J Alloy Compd 504S:S531–S533
30. Kandpal HC, Fecher GH, Felser C (2007) Calculated electronic and magnetic properties of the half-metallic, transition metal based Heusler compounds. J Phys D Appl Phys 40:1507–1523
31. Block T, Carey MJ, Gurney BA, Jepsen O (2004) Band-structure calculations of the half-metallic ferromagnetism and structural stability of full- and half-Heusler phases. Phys Rev B 70:205114-1–205114-5
32. Kudryavtsev YV, Lee YP, Yoo YJ, Seo MS, Kim JM, Hwang JS, Dubowik J, Kim KW, Choi EH, Prokhnenko O (2012) Transport properties of Co_2CrAl Heusler alloy films. Eur Phys J B 85:19–25
33. Galanakis I, Dederichs PH, Papanikolaou N (2002) Slater–Pauling behavior and origin of the half-metallicity of the full-Heusler alloys. Phys Rev B 66(17):1744291–1744299
34. Galanakis I (2005) Orbital magnetism in the half-metallic Heusler alloys. Phys Rev B 71:012413
35. Wittmann R, Spindler S, Fischer B, Wagner H, Gerthsen D, Lange J, Brede M, Klöwer J, Schunk P, Schimmel T (1999) Transmission electron microscopic investigation of the microstructure of Fe–Cr–Al alloy. J Mater Sci 34:1791–1798
36. Rai DP, Shankar A, Sandeep, Singh LR, Jamal M, Hashemifar SJ, Ghimire MP, Thapa RK (2012) Calculation of coulomb repulsion (U) for 3d transition elements in Co_2YAl type Heusler alloys. Armen J Phys 5(3):105–110
37. Gilleßen M, Dronskowski R (2009) A combinatorial study of full Heusler alloys by first-principles computational methods. J Comput Chem 30(8):1290–1299
38. Giannozzi P, Baroni S, Bonini N, Calandra M, Car R, Cavazzoni C, Ceresoli D, Chiarotti GL, Cococcioni M, Dabo I, Dal Corso A, Fabris S, Fratesi G, de Gironcoli S, Gebauer R, Gerstmann U, Gougoussis C, Kokalj A, Lazzeri M, Martin-Samos L, Marzari N, Mauri F, Mazzarello R, Paolini S, Pasquarello A, Paulatto L, Sbraccia C, Scandolo S, Sclauzero G, Seitsonen AP, Smogunov A, Umari P, Wentzcovitch RM (2009) QUANTUM ESPRESSO : a modular and open-source software project for quantum simulations of materials. J Phys Condens Matter 21:395502
39. Perdew JP, Burke K, Ernzerhof M (1996) Generalized gradient approximation made simple. Phys Rev Lett 77:3865–3868
40. Methfessel M, Paxton AT (1989) High-precision sampling for Brillouin-zone integration in metals. Phys Rev B 40:3616–3621
41. Baroni S, Giannozzi P, Testa A (1987) Green's-function approach to linear response in solids. Phys Rev Lett 58(18):1861–1864
42. Baroni S, de Gironcoli S, Dal Corso A, Giannozzi P (2001) Phonons and related crystal properties from density-functional perturbation theory. Rev Mod Phys 73:515–562
43. Isaev E (2009) qha: calculation of thermodynamic properties using the Quasi-Harmonic approximation http://qha.qe-forge.org. Accessed 22 Jul 2013
44. Srivastava GP (1990) The physics of phonons. Adam Hilger, Bristol
45. Murnaghan FD (1944) The compressibility of media under extreme pressures. Proc Natl Acad Sci USA 30(9):244–247
46. Wurmehl S, Fecher GH, Kroth K, Kronast F, Dürr HA, Takeda Y, Saitoh Y, Kobayashi K, Lin HJ, Schönhense G, Felser C (2006) Electronic structure and spectroscopy of the quaternary Heusler alloy $Co_2Cr_{1-x}Fe_xAl$. J Phys D Appl Phys 39:803–815
47. Kudryavtsev YV, Uvarov VN, Oksenenko VA, Lee YP, Kim JB, Hyun YH, Kim KW, Rhee JY, Dubowik J (2008) Effect of disorder on various physical properties of Co_2CrAl Heusler alloy films: experiment and theory. Phys Rev B 77:195104-1–195104-9
48. Bayhan U, Arıkan N, Uğur Ş, Uğur G, Çivi M (2010) Structural, electronic and phonon properties of MoTa and MoNb: a density functional investigation. Physica Scripta 82:015601
49. Born M, Huang K (1954) Dynamical theory of crystal lattices. Clarendon, Oxford
50. M. Gilleßen (2009) Maßgeschneidertes und Analytik-Ersatz: über die quantenchemischen Untersuchungen einiger ternärer intermetallischer Verbindungen. Ph. D. Dissertation, RWTH Aachen University
51. Zayak AT, Entel P, Rabe KM, Adeagbo WA, Acet M (2005) Anomalous vibrational effects in nonmagnetic and magnetic Heusler alloys. Phys Rev B 72:054113-1–054113-8